Dust in the Wind: the Role of Recent Mass Loss in Long Gamma-Ray Bursts

Citation	Margutti, R., Guidorzi, C., Lazzati, D., Milisavljevic, D., Kamble, A., Laskar, T., ... & Soderberg, A. M. (2015). Dust in the Wind: the Role of Recent Mass Loss in Long Gamma-Ray Bursts. The Astrophysical Journal, 805(2), 159. doi:10.1088/0004-637X/805/2/159
DOI	10.1088/0004-637X/805/2/159
Publisher	IOP Publishing
Version	Version of Record
Terms of Use	http://cdss.library.oregonstate.edu/sa-termsofuse

The Astrophysical Journal, 805:159 (6pp), 2015 June 1 doi:10.1088/0004-637X/805/2/159

DUST IN THE WIND: THE ROLE OF RECENT MASS LOSS IN LONG GAMMA-RAY BURSTS

R. Margutti[1], C. Guidorzi[2], D. Lazzati[3], D. Milisavljevic[1], A. Kamble[1], T. Laskar[1], J. Parrent[1], N. C. Gehrels[4], and A. M. Soderberg[1]
[1] Harvard-Smithsonian Center for Astrophysics, 60 Garden St., Cambridge, MA 02138, USA
[2] Department of Physics and Earth Sciences, University of Ferrara, via Saragat 1, I-44122, Ferrara, Italy
[3] Department of Physics, Oregon State University, 301 Weniger Hall, Corvallis, OR 97331, USA
[4] NASA Goddard Space Flight Center, Greenbelt, MD 20771, USA
Received 2014 October 10; accepted 2015 April 5; published 2015 May 29

ABSTRACT

We study the late-time ($t > 0.5$ days) X-ray afterglows of nearby ($z < 0.5$) long gamma-ray bursts (GRBs) with *Swift* and identify a population of explosions with slowly decaying, super-soft (photon index $\Gamma_x > 3$) X-ray emission that is inconsistent with forward shock synchrotron radiation associated with the afterglow. These explosions also show larger-than-average intrinsic absorption ($\mathrm{NH}_{x,i} > 6 \times 10^{21}$ cm^{-2}) and prompt γ-ray emission with extremely long duration ($T_{90} > 1000$ s). The chance association of these three rare properties (i.e., large $\mathrm{NH}_{x,i}$, super-soft Γ_x, and extreme duration) in the same class of explosions is statistically unlikely. We associate these properties with the turbulent mass-loss history of the progenitor star that enriched and shaped the circumburst medium. We identify a natural connection between $\mathrm{NH}_{x,i}$, Γ_x, and T_{90} in these sources by suggesting that the late-time super-soft X-rays originate from radiation reprocessed by material lost to the environment by the stellar progenitor before exploding (either in the form of a dust echo or as reprocessed radiation from a long-lived GRB remnant), and that the interaction of the explosion's shock/jet with the complex medium is the source of the extremely long prompt emission. However, current observations do not allow us to exclude the possibility that super-soft X-ray emitters originate from peculiar stellar progenitors with large radii that only form in very dusty environments.

Key words: gamma-ray burst: general – gamma-ray burst: individual (GRBs 060218, 100316D, 980425, 130925A) – supernovae: general

1. INTRODUCTION

The effects of binarity and the role of mass loss in the decades to years preceding the terminal explosion are among the least understood aspects of massive stellar evolution (e.g., Langer 2012; Smith 2014 for recent reviews). This lack of understanding is significant in light of recent observations showing that more than 70% of massive O-type stars in the Galaxy interact with a binary companion (Sana et al. 2012) and that the classical picture of mass loss through steady winds does not apply to all massive stars, especially during the very last stages of evolution (e.g., Ofek et al. 2013; Margutti et al. 2014a and references therein).

Long gamma-ray bursts (GRBs) are thought to represent the endpoints of the evolution of massive stars that managed to lose their hydrogen envelope before exploding, while retaining enough angular momentum to power a relativistic jet (e.g., MacFadyen & Woosley 1999; MacFadyen et al. 2001). The observed connection of long GRBs with Type Ic supernovae (SNe) and their locations within the host galaxies (Fruchter et al. 2006) strongly support their association with massive stars and are consistent with the suggested Wolf–Rayet (WR) progenitors (see Hjorth & Bloom 2012 for a recent review). However, it is unclear if the progenitors of GRBs are single massive stars or binaries. The rate and the nature of the mass loss (e.g., steady winds versus explosive ejection of shells of material) suffered by the stellar progenitor in the final phases of its evolution before collapsing are also unclear.

Observations are now starting to reveal the turbulent life of some massive stars in the years before the SN explosion and are pointing to the presence of a common (and unexpected) eruptive behavior preceding the collapse (e.g., Ofek et al. 2014; Smith 2014). As a result, the local SN environment is shaped and "enriched" by successive mass ejections. This kind of behavior might be common in GRB progenitor stars as well. In particular, it is relevant to mention (i) the recent report of a possible outburst of the progenitor of the SN Ic PTF11qcj ~2 yr before the SN (Corsi et al. 2014), (ii) the signature of increased mass loss shortly before the explosion of the hydrogen-stripped SNe 2013cu (Gal-Yam et al. 2014) and 2008D (Svirski & Nakar 2014), (iii) the finding of unusual environments around some SNe Ib/SNe Ic as revealed by radio observations (e.g., Berger et al. 2003; Soderberg et al. 2006a, 2006c; Wellons et al. 2012; Bietenholz et al. 2014).

It is thus likely that a complex environment sculpted by the recent mass loss of the progenitor system surrounds GRBs at the time of their explosions. The interaction of the GRB jet and the SN ejecta with this material is expected to leave detectable signatures in their temporal and spectral evolution. Here we present a study of GRBs in the low-redshift universe ($z < 0.5$) that aims to test this hypothesis. We identify a class of explosions with peculiar prompt γ-ray emission and late-time X-ray spectrum and connect these properties with the mass-loss history of their progenitors.

Throughout the paper we use the convention $F_\nu(\nu, t) \propto \nu^{-\beta} t^{-\alpha}$, where the spectral energy index is related to the spectral photon index by $\Gamma = 1 + \beta$. We employ standard cosmology with $H_0 = 71\,\mathrm{km\,s^{-1}\,Mpc^{-1}}$, $\Omega_\Lambda = 0.73$, and $\Omega_\mathrm{M} = 0.27$. Quantities are listed in the cosmological rest-frame of the explosion unless explicitly noted.

Table 1
Prompt Emission and Late-time X-Ray Emission Parameters

GRB	z	$T_{90,\ obs}$ (s)	$NH_{x,i}$ (10^{22} cm^{-2})	Γ_x	α_x	NH_{MW} (10^{22} cm^{-2})
060218	0.0331	2100 ± 100[a]	0.74 ± 0.14	5.5 ± 0.2	1.20 ± 0.08	0.140
060512	0.443[h]	11.4 ± 4.1	<0.054	2.0 ± 0.2	1.68 ± 0.47	0.016
060614	0.125	109.2 ± 3.4	<0.027	1.69 ± 0.04	1.83 ± 0.04	0.020
061021	0.346	43.8 ± 5.6	0.046 ± 0.024	1.94 ± 0.04	1.10 ± 0.03	0.055
090417B	0.345	>2130[b]	2.4 ± 0.4	3.7 ± 0.2	0.87 ± 0.08	0.017
091127	0.490	7.4 ± 0.2	0.084 ± 0.05	1.67 ± 0.04	1.62 ± 0.04	0.031
100316D	0.0590	>1300[c]	0.68 ± 0.02[d]	3.5 ± 0.3[d]	0.87 ± 0.08	0.101
120422A	0.283	5.4 ± 1.4	<0.076	1.7 ± 0.2	0.87 ± 0.11	0.042
130427A	0.340	276.0 ± 5.0[e]	0.040 ± 0.004	1.60 ± 0.02	1.34 ± 0.01	0.019
130702A	0.145	59.0[f]	0.062 ± 0.021	1.72 ± 0.03	1.00 ± 0.02	0.018
130831A	0.4791	32.5 ± 2.5	<0.050	1.7 ± 0.2	1.44 ± 0.35	0.057
130925A	0.347	>7000[g]	2.05 ± 0.20	3.65 ± 0.03	0.79 ± 0.02	0.018

Note. 90% c.l. uncertainties are provided for $NH_{x,i}$. All other uncertainties are 1σ. Upper limits are 3σ.
[a] From Campana et al. (2006).
[b] From Holland et al. (2010).
[c] From Starling et al. (2011).
[d] From Margutti et al. (2013a).
[e] From Maselli et al. (2014).
[f] From Collazzi & Connaughton (2013), 50–300 keV band.
[g] This event has been classified as ultra-long, with a total duration of the prompt emission of ~20 ks (Evans et al. 2014) and γ-rays lasting ~7 ks (Piro et al. 2014).
[h] The redshift of this burst has been disputed by Fynbo et al. (2009). These authors suggest $z = 2.1$ based on the assumed association of a broad absorption line in the afterglow spectrum of GRB 061512 with Lyα. Here we follow the analysis by Bloom et al. (2006). We note that our major conclusions are not sensitive to this particular choice.

2. SAMPLE SELECTION AND DATA ANALYSIS

We study the late-time ($0.5 < t < 10$ days, rest-frame) X-ray emission of nearby ($z < 0.5$) long GRBs. At this epoch the X-rays are expected to be dominated by afterglow synchrotron emission produced as the explosion shock is decelerated by the interaction with the circumburst medium, whereas X-ray flares, steep decays, and plateaus dominate at much earlier epochs (e.g., Margutti et al. 2013b).

We select our sample of GRBs based on the following requirements: (i) redshift measurement, either from the optical afterglow or from unambiguous association to the host galaxy; (ii) bright early-time ($t < 0.5$ days, rest-frame) X-ray emission to extract a spectrum and constrain the intrinsic neutral hydrogen absorption column $NH_{x,i}$; (iii) enough late-time ($0.5 < t < 10$ days, rest-frame) count statistics to constrain the X-ray spectral photon index Γ_x; (iv) limited Galactic absorption along the line of sight $NH_{MW} \lesssim 10^{21}$ cm^{-2} to reliably constrain $NH_{x,i}$ and avoid important contamination from Galactic material.[5] Note that we do not require the GRBs to have been detected by the *Swift* Burst Alert Telescope (BAT, Barthelmy et al. 2005). What we require is an X-ray follow up of the bursts both at early and late times. At the time of writing, only the *Swift* X-ray Telescope (XRT, Burrows et al. 2005) can provide early time X-ray follow up.

Furthermore, we require the GRBs to be at low redshift $z < 0.5$ (i) to sample both extremes of the distribution of $NH_{x,i}$ values (at higher redshift the effective instrumental bandpass sensitive to intrinsic X-ray absorption decreases, thus reducing our ability to measure low $NH_{x,i}$ values, (e.g., Margutti et al. 2013b, their Figure 5); (ii) to minimize the effects of the detector sensitivity and band-pass when measuring the GRB prompt emission duration T_{90} (e.g., Littlejohns et al. 2013); (iii) to sample the soft X-ray emission at $E \lesssim 0.5$ keV in the burst rest-frame. This last requirement is essential to detect additional spectral components to the standard afterglow emission that could otherwise be missed in higher-z GRBs if intrinsically soft. An example in this respect is the blackbody component with $kT_{BB} \sim 0.5$ keV that has been recently reported by Piro et al. (2014) in the late-time X-ray emission of GRB 130925A at $z = 0.347$.

Twelve GRBs satisfy the selection criteria above (Table 1). *Swift*-XRT data have been reduced as we describe in Margutti et al. (2013b), using the latest software and calibration files. Comparison with the online *Swift*-XRT catalog (Evans et al. 2009, 2010) reveals a good agreement. For each GRB we measure the intrinsic absorption $NH_{x,i}$ from a spectrum extracted at $t < 0.5$ days rest-frame, during a time interval where no spectral evolution is apparent. The Galactic contribution in the direction of the burst NH_{MW} is estimated from Kalberla et al. (2005). We constrain the late-time spectral photon index Γ_x by extracting a spectrum in the time interval $0.5 < t < 10$ days, rest-frame, while we estimate the power-law index of the temporal decay α_x by fitting the X-ray light curve in the same time interval. All the spectra have been modeled with an absorbed power-law (*tbabs*ztbabs*pow* within *Xspec*). The duration of the burst prompt emission T_{90} is taken from Sakamoto et al. (2011), *Swift* BAT refined circulars, or dedicated papers.

The results from this analysis are listed in Table 1 and plotted in Figures 1 and 2 (filled stars). We add for completeness the two pre-*Swift* GRBs that would pass our selection criteria, GRBs 980425 and 030329 (open stars). Data have been collected from Tiengo et al. (2003), Kouveliotou

[5] Existing maps of the projected spatial distribution of NH_{MW} like those presented in Kalberla et al. (2005) are not able to capture possible variations of NH_{MW} on small angular scales.

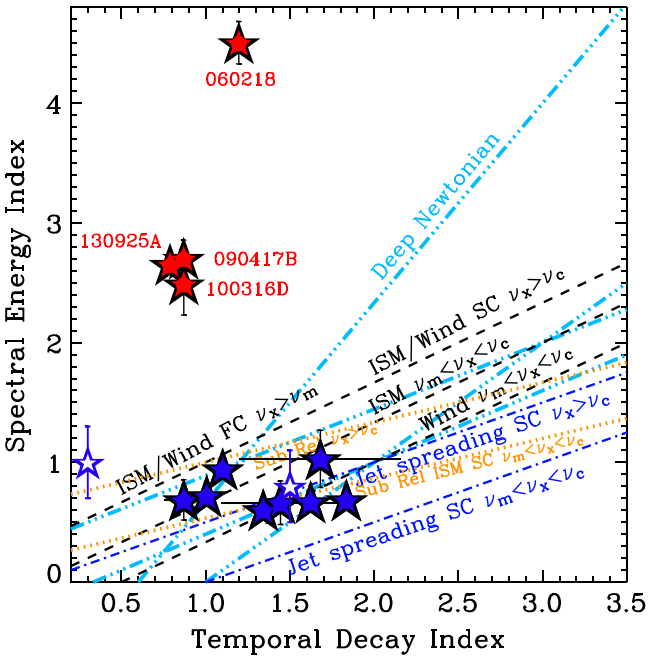

Figure 1. Late-time (0.5–10 days, rest frame) spectral energy index β_x vs. temporal decay index α_x for the sample of nearby GRBs (filled stars). Lines: expectations from synchrotron radiation from a relativistic, sub-relativistic, or newtonian shock expanding into an ISM or wind-like medium (see Margutti et al. 2013a and references therein). GRBs with evidence for super-soft X-ray emission are in red. Open stars: pre-*Swift* GRBs that satisfy the selection criteria of Section 2, i.e., GRBs 980425 and 030329.

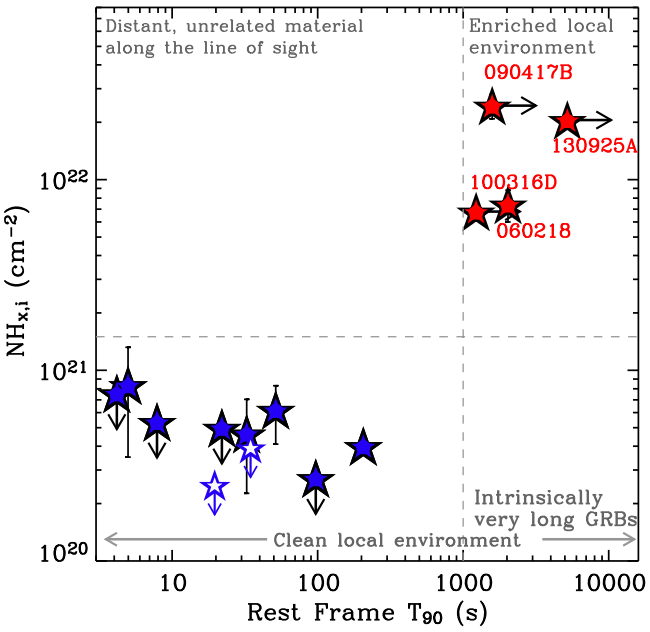

Figure 2. Intrinsic hydrogen column density vs. prompt duration for the sample of nearby GRBs. Red stars: GRBs with evidence for super-soft X-ray emission at late times. Open stars: pre-*Swift* GRBs that satisfy the selection criteria. The dashed horizontal line marks the peak of the $NH_{x,i}$ probability density distribution of all GRBs detected by *Swift* as of 2014 July 16 (Evans et al. 2009). The vertical dashed line at 1000 s is drawn as a visual guide. 99% of GRBs detected by *Swift*-BAT show a rest-frame $T_{90} < 300$ s.

et al. (2004), and Kaneko et al. (2007). The following discussion will however focus on the *Swift*-XRT sample, only, for the sake of homogeneity.

3. RESULTS

Our analysis identifies a population of nearby GRBs with super-soft ($\Gamma_x > 3$) X-ray emission at late-times (red stars in Figures 1 and 2) that is not consistent with afterglow radiation from the forward shock, as shown in Figure 1. Four bursts belong to this class: GRBs 060218, 090417B, 100316D, and 130925A. Their late-time temporal decay is also shallower than average: $\alpha_x < 1.4$, where $\alpha_x = 1.4$ is the median value for the population of GRBs with known redshift (Margutti et al. 2013a, their Figure 4). This finding alone is suggestive of the presence of an additional X-ray emission component with markedly different spectral properties with respect to the afterglow. Indeed, this was the conclusion from accurate broad-band spectral modeling of the emission from GRBs 060218 (Soderberg et al. 2006b), 090417B (Holland et al. 2010), 100316D (Margutti et al. 2013a), and more recently, 130925A (Bellm et al. 2014; Evans et al. 2014; Piro et al. 2014).

Remarkably, we find that the class of late-time super-soft X-ray emitters (red, filled stars) also shows significantly larger intrinsic absorption $NH_{x,i}$ and exceptionally long duration of the prompt emission T_{90}, as demonstrated in Figure 2. These bursts are also associated with fairly large intrinsic optical extinction values: for GRBs 130925A and 090417B Evans et al. (2014) and Holland et al. (2010) infer $A_V \approx 2.2$ mag and $A_V > 2.5$ mag, respectively. In the case of GRB 100316D, Olivares et al. (2012) derive $A_V \approx 1.2$ mag, while the intrinsic extinction along the line of sight to GRB 060218 is likely lower ($E(B-V)_{\rm tot} = 0.13 \pm 0.02$ mag, with a dominating Galactic component, Pian et al. 2006).

In the $NH_{x,i}$–T_{90}–Γ_x phase space the 12 nearby GRBs naturally divide into two groups with no apparent continuum in between. The first group comprises GRBs with large intrinsic absorption $NH_{x,i} \gtrsim 7 \times 10^{21}$ cm^{-2}, extremely long prompt emission $T_{90} > 1000$ s and super-soft late-time X-rays $\Gamma_x > 3$. Low $NH_{x,i} < 10^{21}$ cm^{-2} is instead always associated with a harder X-ray spectrum with $\Gamma_x \lesssim 2$, consistent with the predictions of the afterglow model and a shorter T_{90}. We estimate the probability to obtain the observed configuration by chance below.

Every GRB in our sample can be described by three stochastic variables. Each variable has two possible states, "up" or "down," corresponding to large or small values of $NH_{x,i}$, T_{90} and Γ_x, respectively. The observed configuration corresponds to the case where every GRB is either "up-up-up" or "down-down-down," implying that in our system of 12 GRBs only 2 of the $2^3 = 8$ available states are populated. The chance probability that in a system of N elements only $n \leqslant 2$ of the m possible states are occupied is $P = \frac{(2^{N-1}-1)(m-1)+1}{m^{N-1}}$. For $N = 12$ GRBs and $m = 8$, $P = 1.7 \times 10^{-6}$. This calculation assumes equal probabilities for the "up" and "down" state of each variable ($p_{\rm up} = p_{\rm down} = 0.5$), since a priori there is no reason to believe that any of the two states should be favored against the other. If however this is not true and the "up" state is intrinsically less probable with $p_{\rm up} = 1/3$ ($p_{\rm down} = 2/3$) as suggested by the observations, then a Monte Carlo simulation with 10^6 realizations finds $P = 1.3 \times 10^{-4}$. We note that for both calculations we also conservatively counted as "success" those cases where $n = 1$ (i.e., all the events in the same state).

We can thus reject the hypothesis of a chance association with high confidence ($P > 99.99\%$).

We end by commenting on potential observational biases. Any instrumental detection bias would equally affect bursts in low and high $NH_{x,i}$ environments (γ-rays are not sensitive to the $NH_{x,i}$) regardless of their late-time X-ray spectrum (the prompt emission "knows" nothing about the late-time X-ray spectrum). As a result it could not be responsible for the observed $NH_{x,i}$–T_{90}–Γ_x distribution. Our sample is biased toward GRBs with brighter late-time X-ray emission, as we require enough count statistics to extract a spectrum at $0.5 < t < 10$ days (rest-frame): it is however unclear how this would only affect GRBs with short T_{90} and high $NH_{x,i}$ or long T_{90} and low $NH_{x,i}$. We therefore conclude that the observed configuration with two distinct clusters of GRBs in the $NH_{x,i}$–T_{90}–Γ_x phase space is physically driven.

4. DISCUSSION

4.1. The Γ_x–T_{90}–$NH_{x,i}$ Phase Space

In the collapsar model of long GRBs (MacFadyen et al. 2001) the duration of the prompt emission reflects the central engine activity, with no expected connection with the amount of circumburst material or the spectral properties of the late-time X-ray emission. Our results indicate instead that nearby GRBs do not populate the $NH_{x,i}$–T_{90}–Γ_x phase space randomly, and that these parameters are in some way physically linked. In particular, it suggests that for the super-soft X-ray emitters the measured $NH_{x,i}$ is dominated by material that is directly connected with the explosion and/or progenitor, as opposed to more distant material that just happens to be along our line of sight.

The extreme X-ray softness of the late-time emission of some GRBs has been noticed before (Fan et al. 2006; Soderberg et al. 2006b; Holland et al. 2010; Margutti et al. 2013a; Barniol Duran et al. 2014; Evans et al. 2014; Piro et al. 2014; Zhao & Shao 2014). While there is general agreement on the need for an extra, super-soft X-ray component in addition to the afterglow, different ideas have been proposed to explain its origin.

(i) Radiation from a long-lived GRB central engine, later reprocessed by material in the burst surroundings before reaching the observer (Fan et al. 2006; Soderberg et al. 2006b; Margutti et al. 2013a, see however Barniol Duran et al. 2014).

(ii) Thermal emission from a hot ($kT_{\rm BB} \sim 0.5$ keV) and relatively compact ($R \sim 10^{11}$ cm) cocooon that develops as a result of the interaction of the jet with the stellar layers. This model was specifically developed for GRB 130925A (Piro et al. 2014) but it is supposed to embrace the entire class of GRBs with ultra-long prompt emission (see e.g., Gendre et al. 2013 for details about ultra-long GRBs). This picture connects the late-time super-soft X-ray emission with the atypical nature of the progenitor star (a blue super-giant-BSG-instead of a WR star (WRs), whose outer layers power a longer-than-average jet activity, Woosley & Heger 2012), thus explaining the link between $\Gamma_x > 3$ and $T_{90} > 1000$ s. However, this model does not offer a natural explanation for the large $NH_{x,i}$ (BSG progenitors actually have low mass-loss rates $\dot{M} < 10^{-5}\,M_\odot$ yr^{-1} even in super-solar metallicity environments, Vink et al. 2001).

(iii) Alternatively, a localized dust layer at $R_d \sim 30$–80 pc (GRB 090417B, Holland et al. 2010) or at $R_d \sim 80$–2000 pc (GRB 130925A, Evans et al. 2014; Zhao & Shao 2014) can account for both the spectral softness and the large intrinsic hydrogen column. However, there is no reason to expect a longer than average duration of the prompt emission, contrary to what is observed, if the dust sheet is unrelated to the explosion/progenitor.

The key question is how to connect the properties of the very early γ-ray emission, late-time X-ray radiation and local environment density distribution within a coherent physical picture. GRBs that just happen to be seen through a thick but unrelated sheet of material would homogeneously populate the upper part of the $NH_{x,i}$–T_{90} plot (Figure 2), while bursts where the central engine activity is entirely responsible for the duration of the γ-ray emission are expected to reside in the lower part of the diagram, both at short and at long T_{90}.

To explain the observed distribution of GRBs, with two well defined clusters in the Γ_x–$NH_{x,i}$–T_{90} phase space, we envision two scenarios: (i) the duration of all the events is intrinsic (i.e., it indeed reflects the duration of the activity of the GRB engine) and the longest events originate from peculiar progenitors that only form in very dusty environments, or, more likely, (ii) a single physical mechanism is responsible for the simultaneous appearance of the super-soft X-ray emission at late times, extremely long T_{90}, and large $NH_{x,i}$. We expand on this latter possibility below. We consider the first scenario less likely, as it would require a peculiar progenitor with very large radius (to accommodate for the exceptionally long T_{90}) to form in a peculiar dusty environment. However, we note that current observations do not allow us to rule out this possibility.[6]

4.2. The Role of Progenitor Mass Loss in GRBs with Late-time Super-soft X-Rays

WRs with $M \approx 40\,M_\odot$ are considered the most likely progenitors of GRBs (e.g., MacFadyen & Woosley 1999) and progenitor candidates of at least some ordinary hydrogen-poor SNe (i.e., SNe IIb, SNe Ib, and SNe Ic). During the helium burning phase WRs lose mass through powerful winds at the rate of $\dot{M} \sim 10^{-5}\,M_\odot$ yr^{-1} with velocity $v_w \sim 1000$ km s^{-1}. However, during the last $\sim$100–1000 yr, evolved WRs burn heavier elements and the mass-loss rate is not well constrained. As a result, the mass distribution within $\sim 10^{17}$–10^{18} cm is unknown and might strongly deviate from the $\propto 1/r^2$ wind profile. Three recent observational findings are relevant in this respect: (i) the possible eruption of the SN Ic PTF11qcj $\sim$2 yr before the supernova (Corsi et al. 2014); (ii) the indication of increased mass loss with clear WR signatures shortly before the explosion in the very early spectra of the envelope-stripped SN2013cu (Gal-Yam et al. 2014, see also Groh 2014) and the inference of an increased mass-loss in the days before the explosion of SN 2008D (Svirski & Nakar 2014); (iii) the detection of modulated radio emission from nearby envelope-stripped SNe, which is indicative of pre-explosion mass loss variability (Soderberg et al. 2006a; Wellons et al. 2012).

We suggest that the main difference between the two groups of GRBs in Figures 1 and 2 is connected with the distribution

[6] After our work appeared on the archive, the possibility of a larger progenitor star with a dense core engulfed in a low-mass extended envelope has been suggested by Nakar (2015) to explain the γ-ray and UV properties of GRB 060218.

and amount of material in the burst local environment and that the interaction of the explosion's shock and radiation with the medium enriched by substantial mass loss from the progenitor star is the source of the phenomenology observed in GRBs with super-soft X-ray emission.

In particular, we associate the late-time super-soft X-ray emission with reprocessed radiation by material in the burst surroundings. A possibility is a dust echo of the prompt X-rays as it was suggested for GRBs 090417B and 130925A (Holland et al. 2010; Evans et al. 2014). Following Shao et al. (2008) and Shen et al. (2009; their Equation (4)) and noting that the X-ray "plateau" emission decays around $(1-5)\times10^4$ s in the four GRBs with $\Gamma_x > 3$, we find that the dust sheet is roughly located at $R\sim$10–100 pc from the progenitor. Differently from previous works, here we argue that the physical origin of the material around the GRBs with $\Gamma_x > 3$ has to be connected with the mass-loss history of the progenitor system.

The variable mass loss from massive stars during their evolution is known to create a structured wind bubble around the star (and its possible binary companion) with a dense shell at the interface with the ISM (e.g., Moore et al. 2000). The typical radius of the swept-up shell nebula around a WRs at the end of its life is $R \approx 100(\dot{M}_{-6.2}\, v_{3.5}^2 n_0^{-1})^{1/5} t_{6.6}^{3/5}$ pc, with a critical dependence on the main-sequence (MS) mass-loss rate $\dot{M}$, wind velocity v, MS lifetime t and ISM density n (Castor et al. 1975). Here we normalize our variables to $\dot{M} = 10^{-6.2}$ $M_\odot$ yr^{-1}, $v = 10^{3.5}$ km s^{-1}, $t = 10^{6.6}$ yr, and $n = 1$ cm^{-3}, as appropriate for a 35 $M_\odot$ star (e.g., Dwarkadas 2007). Observations show that shell nebulae are present in ∼35% of WRs (Marston 1997) with $R\sim$ tens of parsecs, intriguingly similar to what we infer for the light-echo scenario above. We suggest that the excess of super-soft X-ray radiation at late times is related with the presence of shell nebulae around the progenitors.[7]

The interior structure of the wind bubble is instead determined by the more recent mass-loss history of the progenitor and possibly results from the ejection of massive shells of material that shaped the medium at $R < 1$ pc. We speculate that the interaction of the explosion's jet/shock with material at $R \sim 10^{14}$–10^{16} cm is at least partially responsible for the very long prompt duration ($T_{90} > 1000$ s) in these sources. In the most extreme cases (i.e., weak or absent explosion's jet and/or thick shell of material in the very close environment), the entire γ-ray emission originates from shock/jet break out radiation through a thick shell, as it was proposed for GRBs 060218 and 100316D by Nakar & Sari (2012; see also Bromberg et al. 2011). In this model the T_{90} reflects the properties of the progenitor star—and in particular its radius—or its environment, as opposed to the duration of the central engine activity. For GRBs 060218 and 100316D, Nakar & Sari (2012) obtained a break-out radius $R_b \sim 5\times10^{13}$ cm, much larger than WRs, and pointed to the presence of opaque material thrown by the star before exploding at $R = R_b$.

[7] We emphasize that at this stage it is not possible to rule out the possibility that the excess of super-soft X-rays originates from radiation from a long-lived central engine, later reprocessed by material in the burst environment before reaching the observer. However, the "echo hypothesis" seems more natural as it does not require an extremely long central engine life-time of several days.

4.3. Testable Predictions

If the interaction of the jet with some material is at least partially responsible for the exceptionally long T_{90}, we expect the following: (i) the interaction would suppress the shortest variability timescales originally present; (ii) the GRBs with the hardest prompt emission would belong to the naked-explosion category, and the softest events to the super-soft X-ray emitters, with overlap between the two classes due to the large variation in the intrinsic properties of the explosions (i.e., before the interaction with the medium).

Observations confirm these expectations. GRBs 060218 and 100316D are characterized by very low prompt peak energy values $E_{\rm pk} < 50$ keV (Kaneko et al. 2007; Starling et al. 2011)[8] and show $\Gamma_x > 3$ at late times, while GRB130427A, with peak energy $E_{\rm pk} \sim 1400$ keV during the main emission episode (Maselli et al. 2014), belongs to the naked-explosion category and is the hardest long GRB at $z \lesssim 0.3$. Furthermore, the very smooth, single-peaked temporal structure of the prompt emission of GRBs 060218 and 100316D is clearly in line with the shock break-out scenario (Nakar & Sari 2012), and it is apparent from Figure 1 of Holland et al. (2010) that for GRB 090417B, the shortest variability timescales were not observed ($\delta t_{\rm var} > 10$ s). Finally, it is remarkable that in spite of the excellent statistics GRB 130925A also shows a large minimum variability time-scale $\delta t_{\rm var}^{\rm min} \sim 1$ s (Greiner et al. 2014) with typical values $\delta t_{\rm var} \sim 10-100$ s (Evans et al. 2014, Figure 5). This finding points to a large dissipation radius $R = 2\times10^{14}$ $(\delta t/1\ {\rm s})(\Gamma/30)^2$ cm, consistent with the picture that we propose.

We conclude with two comments. First, at the moment we have no reasons to believe that no GRB will ever populate the lower-right and upper-left corners of the $\mathrm{NH}_{x,i}$ versus T_{90} plot (Figure 2). Instead, we expect chance alignment with thick but unrelated material to happen for a certain fraction of GRBs. At the same time, we cannot exclude the existence of intrinsically very long GRBs exploding in very clean environments in the low-redshift universe. Since there is no obvious observational bias against the detection of these two groups of explosions, we conclude that they must be less common. Future observations are needed to clarify how GRBs populate the $\mathrm{NH}_{x,i}$ versus T_{90} plane. Second, the discovery of low ambient densities around some of the super-soft X-ray emitters as inferred from broad-band modeling of the afterglow emission (see, e.g., GRB 130925A, Evans et al. 2014) is not in contrast with our picture of an environment with a complex density profile, as the general structure around a massive star is that of a low-density medium surrounded by an overdense shell. Furthermore, repeated shell ejections might as well have swept up the material around the progenitor, leaving behind a low-density cavity (in strict analogy with nova shells, see, e.g., Figure 5 in Margutti et al. 2014b).

5. CONCLUSIONS

We have identified a class of GRBs in the low-redshift universe with (i) super-soft late-time X-ray radiation not consistent with the standard afterglow model, (ii) large X-ray

[8] For completeness we report here that the different episodes of emission of GRB 130925A have $E_{\rm pk} = 60$–100 keV as measured from a Band spectrum by Evans et al. (2014). GRB 090417B instead lacks a high-energy follow up at $E > 150$ keV and its spectrum, as detected by the *Swift*-BAT, is consistent with a simple power-law with spectral photon index $\Gamma = 1.9 \pm 0.1$ (Holland et al. 2010).

absorption, and (iii) exceptionally long prompt γ-ray emission duration. We connect these properties with the turbulent mass-loss history of their stellar progenitors that shaped the environment around the explosions. We suggest that the interaction of the explosion's shock/jet and of the emitted radiation with the complex medium is responsible for the anomalous late-time X-ray spectrum and the extremely long duration of the prompt emission in these sources.

The next step in the research is to understand which physical property distinguishes these stellar progenitors from those producing naked explosions. While this is at the moment unclear, we note that the "peculiarity" of the progenitors of this class of explosions might manifest through different properties of their host-galaxies and, especially, of their local environments (e.g., metallicity at the explosion site, star formation rate, dust content, properties of the underlying stellar population). Furthermore, we predict that the remnants of these explosions will be significantly different from the cases of expansion into an undisturbed ISM or wind-like density profile as the more complex structure of the medium will cause a number of reflected and transmitted shocks to go through the explosion's ejecta and the material in the burst surroundings.

It is beyond current capabilities to spatially resolve the remnants of these explosions due to their large distance. Additionally, we will not be able to witness their evolution in real time: the supernova ejecta will interact with the more distant shell on a timescale of >300 yr, and even a powerful jet with $E = 10^{52}$ erg propagating in a wind medium with $\dot{M} = 10^{-5}\,M_{\odot}\ \mathrm{yr}^{-1}$ would need several decades to reach $R = 10$ pc. We will thus need to rely on the increased capabilities of current and near-future optical surveys to localize bursts from their optical afterglow (as it indeed happened for GRB 130702A, Singer et al. 2013) to build the statistical sample of GRBs in the low-redshift universe necessary to understand how they populate the $\mathrm{NH}_{x,i}$ versus T_{90} plane, constrain and contrast the properties of their environments, and test our expectations.

We thank the referee for helpful comments that improved the quality of our work. R.M. is grateful to the Aspen Center for Physics and the NSF Grant #1066293 for hospitality during the completion of this work and for providing a stimulating environment that inspired this project. Support for this work was provided by the David and Lucile Packard Foundation Fellowship for Science and Engineering awarded to A.M.S.

REFERENCES

Barniol Duran, R., Nakar, E., Piran, T., & Sari, R. 2015, MNRAS, 448, 417
Barthelmy, S. D., Barbier, L. M., Cummings, J. R., et al. 2005, SSRv, 120, 143
Bellm, E. C., Barriére, N. M., Bhalerao, V., et al. 2014, ApJL, 784, L19
Berger, E., Kulkarni, S. R., Frail, D. A., & Soderberg, A. M. 2003, ApJ, 599, 408
Bietenholz, M. F., De Colle, F., Granot, J., Bartel, N., & Soderberg, A. M. 2014, MNRAS, 440, 821
Bloom, J., Foley, R. J., Koceveki, D., & Perley, D. 2006, GCN Circ, 5217
Bromberg, O., Nakar, E., & Piran, T. 2011, ApJL, 739, L55
Burrows, D. N., Hill, J. E., Nousek, J. A., et al. 2005, SSRv, 120, 165
Campana, S., Mangano, V., Blustin, A. J., et al. 2006, Natur, 442, 1008
Castor, J., McCray, R., & Weaver, R. 1975, ApJL, 200, L107
Collazzi, A. C., & Connaughton, V. 2013, GCN, 14972, 1
Corsi, A., Ofek, E. O., Gal-Yam, A., et al. 2014, ApJ, 782, 42
Dwarkadas, V. V. 2007, ApJ, 667, 226
Evans, P. A., Beardmore, A. P., Page, K. L., et al. 2009, MNRAS, 397, 1177
Evans, P. A., Willingale, R., Osborne, J. P., et al. 2010, A&A, 519, A102
Evans, P. A., Willingale, R., Osborne, J. P., et al. 2014, MNRAS, 444, 250
Fan, Y.-Z., Piran, T., & Xu, D. 2006, JCAP, 9, 13
Fruchter, A. S., Levan, A. J., Strolger, L., et al. 2006, Natur, 441, 463
Fynbo, J. P. U., Jakobsson, P., Prochaska, J. X., et al. 2009, ApJS, 185, 526
Gal-Yam, A., Arcavi, I., Ofek, E. O., et al. 2014, Natur, 509, 471
Gendre, B., Stratta, G., Atteia, J. L., et al. 2013, ApJ, 766, 30
Greiner, J., Yu, H. F., Krühler, T., et al. 2014, A&A, 568, A75
Groh, J. H. 2014, A&A, 572, 11
Hjorth, J., & Bloom, J. S. 2012, in Gamma-Ray Bursts, ed. C. Kouveliotou, R. A. M. J. Wijers, & S. Woosley (Cambridge: Cambridge Univ. Press), 169
Holland, S. T., Sbarufatti, B., Shen, R., et al. 2010, ApJ, 717, 223
Kalberla, P. M. W., Burton, W. B., Hartmann, D., et al. 2005, A&A, 440, 775
Kaneko, Y., Ramirez-Ruiz, E., Granot, J., et al. 2007, ApJ, 654, 385
Kouveliotou, C., Woosley, S. E., Patel, S. K., et al. 2004, ApJ, 608, 872
Langer, N. 2012, ARA&A, 50, 107
Littlejohns, O. M., Tanvir, N. R., Willingale, R., et al. 2013, MNRAS, 436, 3640
MacFadyen, A. I., & Woosley, S. E. 1999, ApJ, 524, 262
MacFadyen, A. I., Woosley, S. E., & Heger, A. 2001, ApJ, 550, 410
Margutti, R., Soderberg, A. M., Wieringa, M. H., et al. 2013a, ApJ, 778, 18
Margutti, R., Zaninoni, E., Bernardini, M. G., et al. 2013b, MNRAS, 428, 729
Margutti, R., Milisavljevic, D., Soderberg, A. M., et al. 2014a, ApJ, 780, 21
Margutti, R., Parrent, J., Kamble, A., et al. 2014b, ApJ, 790, 52
Marston, A. P. 1997, ApJ, 475, 188
Maselli, A., Melandri, A., Nava, L., et al. 2014, Sci, 343, 48
Moore, B. D., Hester, J. J., & Scowen, P. A. 2000, AJ, 119, 2991
Nakar, E. 2015, arXiv:150300441
Nakar, E., & Sari, R. 2012, ApJ, 747, 88
Ofek, E. O., Sullivan, M., Cenko, S. B., et al. 2013, Natur, 494, 65
Ofek, E. O., Sullivan, M., Shaviv, N. J., et al. 2014, ApJ, 789, 104
Olivares, E. F., et al. 2012, A&A, 539, A76
Pian, E., Mazzali, P. A., Masetti, N., et al. 2006, Natur, 442, 1011
Piro, L., Troja, E., Gendre, B., et al. 2014, ApJL, 790, L15
Sakamoto, T., Barthelmy, S. D., Baumgartner, W. H., et al. 2011, ApJS, 195, 2
Sana, H., de Mink, S. E., de Koter, A., et al. 2012, Sci, 337, 444
Shao, L., Dai, Z. G., & Mirabal, N. 2008, ApJ, 675, 507
Shen, R.-F., Willingale, R., Kumar, P., O'Brien, P. T., & Evans, P. A. 2009, MNRAS, 393, 598
Singer, L. P., Cenko, S. B., Kasliwal, M. M., et al. 2013, ApJL, 776, 34
Smith, N. 2014, ARA&A, 52, 487
Soderberg, A. M., Chevalier, R. A., Kulkarni, S. R., & Frail, D. A. 2006a, ApJ, 651, 1005
Soderberg, A. M., Kulkarni, S. R., Nakar, E., et al. 2006b, Natur, 442, 1014
Soderberg, A. M., Nakar, E., Berger, E., & Kulkarni, S. R. 2006c, ApJ, 638, 930
Starling, R. L. C., Wiersema, K., Levan, A. J., et al. 2011, MNRAS, 411, 2792
Svirski, G., & Nakar, E. 2014, ApJL, 788, L14
Tiengo, A., Mereghetti, S., Ghisellini, G., et al. 2003, A&A, 409, 983
Vink, J. S., de Koter, A., & Lamers, H. J. G. L. M. 2001, A&A, 369, 574
Wellons, S., Soderberg, A. M., & Chevalier, R. A. 2012, ApJ, 752, 17
Woosley, S. E., & Heger, A. 2012, ApJ, 752, 32
Zhao, Y.-N., & Shao, L. 2014, ApJ, 789, 74